Mimicry of the LL-37 N-terminus enhances the activity of short human cathelicidin derivatives

John S. Albin[1,2,3], Dimuthu A. Vithanage[2,3], Corey Johnson[2,3], and Bradley L. Pentelute[1,4-6*]

[1]Department of Chemistry, Massachusetts Institute of Technology, Cambridge, MA, 02139, USA

[2]Division of Infectious Diseases, Massachusetts General Hospital, Boston, MA, 02114, USA

[3]Harvard Medical School, Boston, MA, 02115, USA

[4]The Koch Institute for Integrative Cancer Research, Massachusetts Institute of Technology, Cambridge, MA 02142, USA

[5]Center for Environmental Health Sciences, Massachusetts Institute of Technology, Cambridge, MA 02139, USA

[6]Broad Institute of MIT and Harvard, Cambridge, MA 02142, USA

*Correspondence: jalbin@mgh.harvard.edu

Summary: Host defense peptides (HDPs) have long been studied as templates for the development of new antibiotic classes, and human HDPs hold unique potential among possible templates due to the evolution of the template peptide as part of the broader human immune system. In this work, we describe the development of lead peptidomimetics based on the human HDP LL-37. Using automated flow peptide synthesis technology, we rapidly generated a series of peptides and peptidomimetics based on our prior structure-activity work in the full-length LL-37 template, which led to the discovery of a modified minimal unit of LL-37 in which potency is enhanced by appending an N-terminal biphenyl clamp from the native sequence to the previously described core activity region. Activity of this lead derivative, termed FF-14, was further improved through the application of D-amino acids and C-terminal amidation as well as selected N-lipidation moieties to the template sequence, providing the foundation for future iteration on a small, highly active derivative of LL-37.

Keywords: LL-37, cathelicidin, antimicrobial peptide, host defense peptide, Pseudomonas, antibiotic, peptide, peptidomimetic

Introduction

Antimicrobial resistance is a growing threat to human health, accounting for 1.2 million deaths in 2019[1]. Absent the development of new antibiotics, this death toll is expected to escalate in the coming decades[2]. One approach to the development of new antibiotics is to develop derivatives of host defense peptides (HDPs), which are structurally diverse miniproteins produced by all branches of life to defend against microbes[3,4]. Although a number of technical barriers have stymied efforts to develop new antibiotics based on HDP scaffolds over the years, these remain a promising starting point for the development of new classes of antibiotics, as the sequence space occupied by synthetic peptides and peptidomimetics offers vast chemical diversity in the context of a chemical scaffold that is typically more chemically tractable than that involved in the development of more synthetically complex natural products. Our own interest in this topic, for example, stems primarily from the development of methods for the synthesis of hypervariable quintillion-member polyamide libraries that may permit the efficient exploration of vastly greater quantities of combinatorial chemical space than can be practically achieved using more traditional methods[5].

Among HDPs, human HDPs hold particular promise as templates for further development due to the home field advantage of having evolved in the context of the human immune system, meaning both that the starting sequence of such templates is inherently nonimmunogenic and that these starting templates may have natural immunomodulatory activities that may contribute to the clearance of an infection[6,7]. The most studied of these human antimicrobial peptides is the lone human cathelicidin, LL-37, a product of neutrophils and other cell types, which in its active form is a 37-residue helical peptide with potent activity against gram-negative bacteria and a wide range of proposed immunomodulatory functions[8–14]. Many prior reports describe the activities of diverse fragments of LL-37, though none of these have ultimately resulted in the development of an antibiotic class that has advanced through the regulatory process[15].

A number of factors have limited the development of LL-37 and other antimicrobial peptides as therapeutics. Stability is a common issue with peptide therapeutics, though it is also one for which viable workarounds exist, such as stapling[16,17], primary sequence changes, and peptidomimetic alterations including the use of D- amino acids that are not recognized by native L-proteases[18]. Many antimicrobial peptides have relatively limited potency, though others such as LL-37 start from a low-micromolar range of activity in the native peptide and may be amenable to further development. Mammalian cell toxicity related to the incomplete selectivity of membranolytic peptides for bacterial over mammalian cells is another limiting factor, which can be difficult to fully ablate even in highly optimized sequences[19,20].

Here, we report the development of lead peptidomimetics based on LL-37. Starting from our prior work on structure-activity relationships in the full-length LL-37 template, we find that mimicry of the LL-37 N-terminus by transposing a biphenyl clamp to the previously described core activity region[21] substantially improves the potency of a short derivative of LL-37, which we have termed FF-14. Additional strategies including perfluoroaryl stapling, the use of D- amino acids chemically inert to native L-proteases, C-terminal amidation, and the use of selected N-lipidation moieties demonstrate additional potential for improving FF-14 potency against gram-negative bacteria. We anticipate that further peptidomimetic development in the context of the FF-14 template, particularly the incorporation of detoxification strategies that we have developed in the context of full-length LL-37 as well as the application of combinatorial library synthesis for improved template discovery, may yield additional improvements to support progress toward a class of clinical viability antimicrobials based on LL-37.

Results

Limited activity of short derivatives of LL-37 against gram-negative bacteria

By convention, peptide derivatives of the human cathelicidin CAMP gene are named according to their first two amino acids and their overall length – thus, LL-37 starts with the amino acids LL and is 37 residues long[22–25]. A large number of studies have previously reported on the activity of diverse fragments of LL-37[15], and among these, KR-12, a 12-residue fragment extending from residues 18-29 of the native peptide, is generally considered the definitive minimal unit of LL-37 activity[21].

The initial description of KR-12 (LL-37 18-29) demonstrates modest potency, with a minimum inhibitory concentration (MIC) of 40 µM against *E. coli* K12, which in those studies was equivalent to the MICs seen with another derivative, FK-13[26,27], as well as wild-type LL-37. By contrast, most approved antibiotics active against gram-negative bacteria have Clinical & Laboratory Standards Institute (CLSI) MIC cutoffs in the single-digit micromolar range[28]. Thus, although KR-12 is the shortest unit of LL-37 activity, its overall potency is somewhat lower than is likely to be required in order to eventually derive clinically useful antimicrobials from LL-37 templates. Even FK-13, which is slightly more potent than KR-12 in most studies but still relatively non-toxic, is borderline. We therefore sought to identify short derivatives of LL-37 with greater potency, from which we might then apply structure-activity approaches such as those that we have used to detoxify full-length LL-37 while conserving antimicrobial activity.

To revisit the subject of shorter derivatives of LL-37 closer in size to approved antimicrobial natural products such as daptomycin and colistin, we made a series of fragments of LL-37 based on prior studies and assessed their relative activity against *E. coli* and *Pseudomonas* as well as their hemolytic activity against defibrinated sheep blood. Among these fragments, all except LL-25, GD-23, FK-13, and full-length LL-37 demonstrated MICs greater than assay against *E. coli*, indicative of generally low levels of antimicrobial activity (**Figure 1A**). Similar results were seen with *Pseudomonas* in **Figure 1B**, albeit with generally lower activity

across active derivatives within assay. Consistent with generally low levels of antimicrobial activity, most derivatives demonstrated little to no hemolytic activity in **Figure 1C**, the major exception being LL-37. An alignment of these initial derivatives is shown in **Figure 1D**. Thus, while many LL-37 derivatives show low toxicity to mammalian cell membranes, these generally also lack potent activity against gram-negative bacteria, limiting their utility as starting points for the development of new antibiotics based on the LL-37 scaffold. The major exceptions to this are LL-25 and GD-23, each of which is reasonably efficient at separating hemolytic function from antimicrobial activity. Although not developed further in this study, these may prove to be favorable templates for the development of small derivatives distinct from those described here. We note, for example, that both LL-25 and GD-23 omit a portion of the LL-37 sequence that we have recently found to be important both for oligomerization and for global membrane permeabilization activity. It is possible that separation of function occurs in these truncation mutants by the same mechanism. **Supplementary Figure 1** provides a histogram depiction of the data in **Figure 1** including error bars. **Supplementary Figures 2-14** (antimicrobial susceptibility) and **15-27** (hemolysis) show the kinetic growth and hemolysis curves associated with each experimental endpoint depicted in **Figure 1**. **Supplementary Table 1** provides a standard, quantitative summary of the results in **Figure 1**.

Mimicry of the LL-37 N-terminus improves the potency of 14-mer derivatives of LL-37

Among the studies in **Figure 1**, three observations stood out to us. First, the most active candidates in **Figure 1** tended to include greater proportions of the LL-37 N-terminus, which is consistent with surface mutagenesis of LL-37 that we have previously completed, in which grouped Ala mutagenesis of the LL-37 N-terminus ablates LL-37 activity against gram-negative bacteria despite being distant in linear sequence from the putative core activity region surrounding LL-37 residues 18-29. One of these surface mutagenesis derivatives, in particular, has no mutations within the core activity region, but is notable for the presence of a biphenyl

clamp motif. In wild-type LL-37, the four native Phe residues are thought to be primary mediators of membrane interaction, and conserved aromatic residues are also found among α defensins[21,29]. We further noted that the inclusion of N-terminal Phe in FK-13 yielded improved activity over the KR-12 minimal unit (**Figure 1**). We therefore reasoned that transposition of the LL-37 N-terminal biphenyl motif, FF[RK], to the N-terminus of KR-12, [KR], might yield a short derivative of LL-37 with improved activity.

To test this hypothesis, we made derivatives FF-14 and FF-14-RK, in which the N-terminal biphenyl clamp of LL-37 was transposed onto the central KR-12 region. As shown in **Figures 2A-B**, this results in 14-mer derivatives of LL-37 that more closely mimic the antimicrobial activities of wild-type LL-37, including potency at least 16-times greater than KR-12 and 4-times greater than FK-13, safely into low micromolar MIC ranges closer to those of many approved antibiotics. Although this comes at a cost of increased hemolysis relative to KR-12 / FK-13, hemolysis among these 14-mers remained 4-8 times less than LL-37 (**Figure 2C**); no substantial differences were noted based on the ordering of [KR] within this motif. We therefore considered that FF-14 might more faithfully recapitulate the activity of LL-37 when used as a lead scaffold for antimicrobial development and opted to explore further alterations to this short derivative of LL-37. The sequences of these and other derivatives tested are shown in **Figure 2D**.

D-amino acids and C-terminal amidation improve FF-14 potency

A number of peptidomimetic alterations have been demonstrated previously to stabilize and improve upon the native activities of HDP scaffolds such as D-amino acids and end modifications (*e.g.*. [26,30,31] among examples with LL-37 and derivatives thereof). To determine whether similar alterations could improve the activity of FF-14, we made an expanded set of peptidomimetic derivatives in which FF-14 was either changed to an all-D configuration or amidated at the C-terminus. As shown in **Figure 2A-B**, enantiomeric ff-14 and C-amidated FF-

14 each demonstrated modest improvements in antimicrobial activity, particularly in *E. coli*, with slightly less hemolytic activity for the all-D ff-14 derivative than wild-type LL-37. It may therefore be possible to improve upon derivatives of FF-14 through stabilizing mutations such as the incorporation of D- amino acids and C-terminal amidation. Of note, activity of FK-13 also improved in all-D format, with retention of the same fold-separation between its 20% hemolysis threshold and MIC. Although retro-inverso fk-13 also retained activity equivalent to all-D fk-14, retro-FK-13 lost activity. **Supplementary Figure 28** provides a histogram depiction of the data in **Figure 2** including error bars. **Supplementary Figures 29-41** (antimicrobial susceptibility) and **42-54** (hemolysis) show the kinetic growth and hemolysis curves associated with each experimental endpoint depicted in **Figure 2**. **Supplementary Table 2** provides a standard, quantitative summary of the results in **Figure 2**.

Perfluoroaryl stapling of LL-37 derivatives improves antimicrobial activity

Despite the improved activity of FF-14 and derivatives thereof that better recapitulated the activity of LL-37, we noted substantial ongoing hemolytic activity that would ultimately preclude the use of LL-37 derivatives without some intervention aimed at decreasing overall toxicity. In related work, we have previously identified I24 and L28 as the primary determinants of mammalian cell toxicity in full-length LL-37, where the incorporation of Ala at these sites largely abrogates membranolytic activity. These residues also occur within the KR-12 core (I9 and L13 in FF-14 numbering), and one of our development strategies has been to use these residues as a starting point for the detoxification of potent, short derivatives of LL-37, as we have done in other work making peptaibol-inspired FF-14 derivatives. We therefore hypothesized that stapling strategies, particularly those involving I9 and L13, might result in similar ablation of toxicity within FF-14.

To test this hypothesis, we made a series of selected perfluoraryl stapled versions of FK-13 as well as a comprehensive set of *i*,*i*+3, *i*,*i*+4, and *i*,*i*+7 perfluoroaryl stapled versions of the

FF-14 hydrophobic surface[16]. The general scheme for stapling at Cys residues under this methodology is shown in **Figure 3**. As shown in **Figures 4A-B**, some of these demonstrated improved activity over the parent peptide, particularly FK-13, but failed to abrogate the hemolytic activity of any derivative demonstrating antimicrobial activity greater than that of FK-13. Similarly, although the Hemo/MIC ratio improves for stapling of FF-14 at V6+I9, the resultant compound has a marked reduction in raw activity. Pilot experiments with lactam and Pd arylation stapling chemistries did not improve upon these results (data not shown). We further noted the tendency of most staples to carry hydrophobic properties comparable to our perfluoroaryl staples, which might ultimately counteract any shielding effect at the hydrophobic surface. Thus, although stapling might ultimately prove a useful modification in another context or perhaps when using other chemistries, we opted not to pursue this further as a means of modulating toxicity in the FF-14 template. **Supplementary Figure 55** provides a histogram depiction of the data in **Figure 4** including error bars. **Supplementary Figures 56-70** (antimicrobial susceptibility) and **71-85** (hemolysis) show the kinetic growth and hemolysis curves associated with each experimental endpoint depicted in **Figure 4**. **Supplementary Table 3** provides a standard, quantitative summary of the results in **Figure 4**.

N-lipidation modulates FF-14 activity

A lipid tail is important for the activity of certain antibiotics such as colistin and daptomycin. Along these lines, prior studies have indicated that certain lipid tails can improve the activity of the KR-12 template[32,33], though often at a cost of toxicity. We reasoned that the same might be true in FF-14. For example, the N-terminal biphenyl clamp in native LL-37 is preceded by two Leu residues – L_1LGDFF_6. We therefore proceeded to test the effects of lipid moieties of several structural types on the antimicrobial and hemolytic activities in FF-14, which in addition to further exploring the theme of N-terminal mimicry for improving the activity of short

LL-37 derivatives also expands upon the list of lipid tails tested in short derivatives of LL-37. Lipid moieties included are shown in **Figure 5**.

As shown in **Figures 6A-B**, the addition of several moieties to the FF-14 N-terminus results in improved antimicrobial activity, though this may differ by species. 5-dimethylamino-pentanoic acid and octanoic acid both improve activity against *E. coli*, octanoic acid proves more potent against *Pseudomonas*. Despite this, 5-dimethylamino-pentanoic acid and derivatives thereof may be useful for limiting the toxic effects of lipid tails based on the ability of this addition to halve the FF-14 MIC while maintaining the same 20% toxicity threshold. Overall, only 5-dimethylamino-pentanoic acid and FF-14 show substantial improvements over wild-type LL-37 in these studies, with most lipidation strategies adversely impacting antimicrobial activity, hemolytic activity, or both, including some that have proven beneficial in other scaffolds such as biphenyl moieties[34]. It may prove beneficial to trial alternative placement of lipid moieties within the FF-14 template, but such studies are beyond the scope of the present work. **Supplementary Figure 86** provides a histogram depiction of the data in **Figure 6** including error bars. **Supplementary Figures 87-102** (antimicrobial susceptibility) and **103-118** (hemolysis) show the kinetic growth and hemolysis curves associated with each experimental endpoint depicted in **Figure 6**. **Supplementary Table 4** provides a standard, quantitative summary of the results in **Figure 6**.

Discussion

In this study, we have described the development of a short derivative of LL-37 comprised of an N-terminal biphenyl clamp transposed onto a previously characterized central activity region from amino acids 18-29. The inclusion of this biphenyl clamp improves the activity of the previously reported minimal unit of LL-37 activity, KR-12. This is consistent with structural data from the same landmark study, which indicated that the four Phe residues of LL-37 are critical for interaction with model membranes[21]. The resultant short derivative, FF-14, more directly mirrors the activity of LL-37, which may make this a useful lead scaffold from which to build out peptidomimetic derivatives. Further work identifies D- amino acids, C-amidation, and N-lipidation as additional strategies for improvement of this template. Although certain stapling combinations, particularly V6+I9, show some ability to separate hemolytic and antimicrobial functions, perfluoroaryl stapling was generally not a fruitful strategy for improving the FF-14 template in our hands, though it is possible that other stapling strategies may differ. This stands in contrast with our recent studies in which we have identified derivatives of LL-37 with markedly decreased hemolytic activity, which localizes primarily to two amino acids. Although these two amino acids separate hemolytic and antibacterial functions in LL-37 and are located in the FF-14 (and FK-13 and KR-12 scaffolds), stapling at these residues did not abrogate hemolytic activity in our studies (see staples involving residues 9 and 13 in **Figure 4** and **Supplementary Table 3**).

Among the lipidation moieties trialed, 5-dimethylamino-pentanoic acid demonstrates modest potential for the separation of antimicrobial activity and hemolytic activity, though this is tempered by its diminished activity against *Pseudomonas*. Further studies may focus on variants of 5-dimethylamino-pentanoic acid. It may also prove beneficial to trial different placement of lipidation moieties within LL-37-derived scaffolds, as even moieties with an apparent neutral or detrimental effect on activity when placed at the N-terminus may behave differently at other sites.

In summary, we describe here a modestly expanded minimal unit of LL-37 activity that better recapitulates the activity patterns of full-length LL-37 through mimicry of the LL-37 N-terminus. We also describe several alterations that may prove beneficial in the development of FF-14 or related scaffolds such as FK-13, including the use of D- amino acids and C-terminal amidation as well as stapling along the hydrophobic face of FF-14 and selected lipidation moieties that improve overall characteristics such as 5-dimethylamino-pentanoic acid.

Despite all of this, the derivatives described in this study are still well short of the *in vitro* therapeutic index displayed by the otherwise toxic comparator antibiotic colistin. Although it may be possible to iterate through various permutations of the above to arrive at something better than FF-14, particularly by combining strategies, the combinatorial matrix quickly becomes daunting. An alternative approach would be to move these same tasks to selection-based drug discovery efforts in which combinatorial libraries based on the FF-14 scaffold are used to select for certain phenotypes such as cell-type selectivity, where a shorter scaffold such as FF-14 is desirable not only for being closer in size to drugs and closer in MIC to approved antibiotics, but also for greater compatibility with mass spectrometric characterization such as *de novo* peptide sequencing[35]. With this is mind, we have recently developed a methodology for the synthesis and deconvolution of extremely large polyamide libraries on the order of up to 10^{18} members[5]. In addition to selected permutations using traditional methods, we anticipate focusing efforts on leveraging the massive combinatorial potential of this system to more efficiently explore chemical space within the FF-14 scaffold, particularly for the purpose of incorporating detoxifying features that we have identified in related studies on the LL-37 and FF-14 templates.

Methods

Antimicrobial susceptibility testing –

Susceptibility testing was carried out based on previously described adaptations of CLSI methods modified further for the use of antimicrobial peptides. This includes the use of polypropylene plates as well as unadjusted Mueller Hinton Broth[36]. Methods were further miniaturized for use in 384-well plates at total volumes of either 35 or 50 µL. In brief, a 10x concentration of peptide was plated followed by the addition of a concentrated medium and cell mixture to yield a 1x mixture of peptide, medium, and cells. For example, if plating 50 µL, one would plate 5 µL of a 10x concentration of peptide followed by 45 µL of a 10/9 strength MHB and cell mixture. Plates were then monitored for absorbance at 600 nm for 18 hours at 37 °C at 30-minute intervals on a Tecan Spark plate reader, during which time they were housed in a large Tecan humidity cassette to minimize evaporation over the course of the experiment. Endpoint measures as depicted in main text figures are the final time point at 18 hours. Growth curves associated with these experiments can be found among the **Supplementary Figures**. Strains used throughout are antimicrobial susceptibility testing quality control strains, namely *E. coli* ATCC 25922 and *Pseudomonas* ATCC 27853.

Hemolysis assays –

Hemolysis assays were carried out by treating defibrinated sheep blood (Hardy Diagnostics) with each test peptide. In brief, peptides were prepared at a concentration of 500 µM in water and then diluted to 400 µM with 5x PBS. These were then serially diluted to the levels shown and plated at 25 µL per well in 384-well plates. To these peptides, we then added 25 µL of sheep blood washed to supernatant clearance for a final concentration of 0.5% v/v. Wells were then monitored at OD600 in a fashion similar to the methods used for antimicrobial susceptibility testing over 18 hours, which provides the kinetic curves shown in the **Supplementary Figures**. At the end of 18 hours, 25 µL of PBS was added to each well

followed by spinning of the 384-well plates for 10 minutes at 800 rcf. 25 µL of supernatant was then removed and added to a fresh 384-well plate for detection of free hemoglobin at 414 nm. Hemolysis controls throughout were thrice free-thawed blood from the same preparation used in plating, which were set to 100%.

Peptide synthesis –

Peptides used in these studies were synthesized on automated flow synthesizers in a manner similar to those previously described[37–40]. Cleavage was generally carried out by treating resin with Reagent K (82.5 % trifluoroacetic acid (TFA), 5% water, 5% phenol, 2.5% 1,2-ethanedithiol) for 2 hours at room temperature followed by precipitation with cold ether. Precipitated peptide was then resuspended in 50% water + 0.1% TFA / 50% acetonitrile + 0.1% TFA and lyophilized. Crude material was purified most commonly by reverse phase flash purification on a Biotage Selekt flash chromatography instrument with selected peptides purified by reverse phase high performance liquid chromatography.

Perfluoroaryl stapling –

Methods for stapling are based on those previously reported (*e.g.*, [16]). Intervals of *I,i+3* or *i,i+4* were stapled using hexafluorobenzene, while intervals of *i,i+7* were stapled with decafluorobiphenyl. In brief, peptide was dissolved to 1 mM in DMF with the addition of stapling agent (2 mM final concentration for decafluorobiphenyl; 20 mM final concentration for hexafluorobenzene) and Tris to a final concentration of 30 mM. Reactions were then allowed to proceed for approximately 4-5 hours prior to dilution in water and purification by reverse phase flash chromatography.

Lipidation –

Lipidation was generally carried out via standard peptide bond formation procedures either in batch or by semi-automated flow synthesis[40] between the on-resin protected peptide and the carboxylic acid on each of the tails used in these studies (**Figure 5**). Cleavage then proceeded as per above for most moieties with selected exceptions for which alternatives such as Reagent B (88% TFA, 5% water, 5% phenol, 2% triisopropylsilane) were substituted.

Acknowledgements

This work has been funded by the National Institute of Allergy and Infectious Diseases (T32 AI007061 and K08 AI166345 to JSA; U19 AI142780 to BLP) and by the Cystic Fibrosis Foundation (ALBIN19F0, ALBIN21Q0, ALBIN22A0-KB to JSA).

Author Contributions

JSA designed and conducted the experiments and wrote the paper. CJ and DAV performed the experiments. BLP guided the experiments and wrote the paper.

Declaration of Interests

JSA declares no competing interests. BLP is a co-founder and/or member of the scientific advisory boards of several companies involved in peptide and protein therapeutics.

References

(1) Murray, C. J.; Ikuta, K. S.; Sharara, F.; Swetschinski, L.; Robles Aguilar, G.; Gray, A.; Han, C.; Bisignano, C.; Rao, P.; Wool, E.; Johnson, S. C.; Browne, A. J.; Chipeta, M. G.; Fell, F.; Hackett, S.; Haines-Woodhouse, G.; Kashef Hamadani, B. H.; Kumaran, E. A. P.; McManigal, B.; Agarwal, R.; Akech, S.; Albertson, S.; Amuasi, J.; Andrews, J.; Aravkin, A.; Ashley, E.; Bailey, F.; Baker, S.; Basnyat, B.; Bekker, A.; Bender, R.; Bethou, A.; Bielicki, J.; Boonkasidecha, S.; Bukosia, J.; Carvalheiro, C.; Castañeda-Orjuela, C.; Chansamouth, V.; Chaurasia, S.; Chiurchiù, S.; Chowdhury, F.; Cook, A. J.; Cooper, B.; Cressey, T. R.; Criollo-Mora, E.; Cunningham, M.; Darboe, S.; Day, N. P. J.; De Luca, M.; Dokova, K.; Dramowski, A.; Dunachie, S. J.; Eckmanns, T.; Eibach, D.; Emami, A.; Feasey, N.; Fisher-Pearson, N.; Forrest, K.; Garrett, D.; Gastmeier, P.; Giref, A. Z.; Greer, R. C.; Gupta, V.; Haller, S.; Haselbeck, A.; Hay, S. I.; Holm, M.; Hopkins, S.; Iregbu, K. C.; Jacobs, J.; Jarovsky, D.; Javanmardi, F.; Khorana, M.; Kissoon, N.; Kobeissi, E.; Kostyanev, T.; Krapp, F.; Krumkamp, R.; Kumar, A.; Kyu, H. H.; Lim, C.; Limmathurotsakul, D.; Loftus, M. J.; Lunn, M.; Ma, J.; Mturi, N.; Munera-Huertas, T.; Musicha, P.; Mussi-Pinhata, M. M.; Nakamura, T.; Nanavati, R.; Nangia, S.; Newton, P.; Ngoun, C.; Novotney, A.; Nwakanma, D.; Obiero, C. W.; Olivas-Martinez, A.; Olliaro, P.; Ooko, E.; Ortiz-Brizuela, E.; Peleg, A. Y.; Perrone, C.; Plakkal, N.; Ponce-de-Leon, A.; Raad, M.; Ramdin, T.; Riddell, A.; Roberts, T.; Robotham, J. V.; Roca, A.; Rudd, K. E.; Russell, N.; Schnall, J.; Scott, J. A. G.; Shivamallappa, M.; Sifuentes-Osornio, J.; Steenkeste, N.; Stewardson, A. J.; Stoeva, T.; Tasak, N.; Thaiprakong, A.; Thwaites, G.; Turner, C.; Turner, P.; van Doorn, H. R.; Velaphi, S.; Vongpradith, A.; Vu, H.; Walsh, T.; Waner, S.; Wangrangsimakul, T.; Wozniak, T.; Zheng, P.; Sartorius, B.; Lopez, A. D.; Stergachis, A.; Moore, C.; Dolecek, C.; Naghavi, M. Global Burden of Bacterial Antimicrobial Resistance in 2019: A Systematic Analysis. *The Lancet* **2022**, *399* (10325), 629–655. https://doi.org/10.1016/S0140-6736(21)02724-0/ATTACHMENT/B227DEB3-FF04-497F-82AC-637D8AB7F679/MMC1.PDF.

(2) Naghavi, M.; Vollset, S. E.; Ikuta, K. S.; Swetschinski, L. R.; Gray, A. P.; Wool, E. E.; Robles Aguilar, G.; Mestrovic, T.; Smith, G.; Han, C.; Hsu, R. L.; Chalek, J.; Araki, D. T.; Chung, E.; Raggi, C.; Gershberg Hayoon, A.; Davis Weaver, N.; Lindstedt, P. A.; Smith, A. E.; Altay, U.; Bhattacharjee, N. V; Giannakis, K.; Fell, F.; McManigal, B.; Ekapirat, N.; Mendes, J. A.; Runghien, T.; Srimokla, O.; Abdelkader, A.; Abd-Elsalam, S.; Aboagye, R. G.; Abolhassani, H.; Abualruz, H.; Abubakar, U.; Abukhadijah, H. J.; Aburuz, S.; Abu-Zaid, A.; Achalapong, S.; Addo, I. Y.; Adekanmbi, V.; Adeyeoluwa, T. E.; Adnani, Q. E. S.; Adzigbli, L. A.; Afzal, M. S.; Afzal, S.; Agodi, A.; Ahlstrom, A. J.; Ahmad, A.; Ahmad, S.; Ahmad, T.; Ahmadi, A.; Ahmed, A.; Ahmed, H.; Ahmed, I.; Ahmed, M.; Ahmed, S.; Ahmed, S. A.; Akkaif, M. A.; Al Awaidy, S.; Al Thaher, Y.; Alalalmeh, S. O.; AlBataineh, M. T.; Aldhaleei, W. A.; Al-Gheethi, A. A. S.; Alhaji, N. B.; Ali, A.; Ali, L.; Ali, S. S.; Ali, W.; Allel, K.; Al-Marwani, S.; Alrawashdeh, A.; Altaf, A.; Al-Tammemi, A. B.; Al-Tawfiq, J. A.; Alzoubi, K. H.; Al-Zyoud, W. A.; Amos, B.; Amuasi, J. H.; Ancuceanu, R.; Andrews, J. R.; Anil, A.; Anuoluwa, I. A.; Anvari, S.; Anyasodor, A. E.; Apostol, G. L. C.; Arabloo, J.; Arafat, M.; Aravkin, A. Y.; Areda, D.; Aremu, A.; Artamonov, A. A.; Ashley, E. A.; Asika, M. O.; Athari, S. S.; Atout, M. M. W.; Awoke, T.; Azadnajafabad, S.; Azam, J. M.; Aziz, S.; Azzam, A. Y.; Babaei, M.; Babin, F.-X.; Badar, M.; Baig, A. A.; Bajcetic, M.; Baker, S.; Bardhan, M.; Barqawi, H. J.; Basharat, Z.; Basiru, A.; Bastard, M.; Basu, S.; Bayleyegn, N. S.; Belete, M. A.; Bello, O. O.; Beloukas, A.; Berkley, J. A.; Bhagavathula, A. S.; Bhaskar, S.; Bhuyan, S. S.; Bielicki, J. A.; Briko, N. I.; Brown, C. S.; Browne, A. J.; Buonsenso, D.; Bustanji, Y.; Carvalheiro, C. G.; Castañeda-Orjuela, C. A.; Cenderadewi, M.; Chadwick, J.; Chakraborty, S.; Chandika, R. M.; Chandy, S.; Chansamouth, V.; Chattu, V. K.; Chaudhary, A. A.;

Ching, P. R.; Chopra, H.; Chowdhury, F. R.; Chu, D.-T.; Chutiyami, M.; Cruz-Martins, N.; da Silva, A. G.; Dadras, O.; Dai, X.; Darcho, S. D.; Das, S.; De la Hoz, F. P.; Dekker, D. M.; Dhama, K.; Diaz, D.; Dickson, B. F. R.; Djorie, S. G.; Dodangeh, M.; Dohare, S.; Dokova, K. G.; Doshi, O. P.; Dowou, R. K.; Dsouza, H. L.; Dunachie, S. J.; Dziedzic, A. M.; Eckmanns, T.; Ed-Dra, A.; Eftekharimehrabad, A.; Ekundayo, T. C.; El Sayed, I.; Elhadi, M.; El-Huneidi, W.; Elias, C.; Ellis, S. J.; Elsheikh, R.; Elsohaby, I.; Eltaha, C.; Eshrati, B.; Eslami, M.; Eyre, D. W.; Fadaka, A. O.; Fagbamigbe, A. F.; Fahim, A.; Fakhri-Demeshghieh, A.; Fasina, F. O.; Fasina, M. M.; Fatehizadeh, A.; Feasey, N. A.; Feizkhah, A.; Fekadu, G.; Fischer, F.; Fitriana, I.; Forrest, K. M.; Fortuna Rodrigues, C.; Fuller, J. E.; Gadanya, M. A.; Gajdács, M.; Gandhi, A. P.; Garcia-Gallo, E. E.; Garrett, D. O.; Gautam, R. K.; Gebregergis, M. W.; Gebrehiwot, M.; Gebremeskel, T. G.; Geffers, C.; Georgalis, L.; Ghazy, R. M.; Golechha, M.; Golinelli, D.; Gordon, M.; Gulati, S.; Gupta, R. Das; Gupta, S.; Gupta, V. K.; Habteyohannes, A. D.; Haller, S.; Harapan, H.; Harrison, M. L.; Hasaballah, A. I.; Hasan, I.; Hasan, R. S.; Hasani, H.; Haselbeck, A. H.; Hasnain, M. S.; Hassan, I. I.; Hassan, S.; Hassan Zadeh Tabatabaei, M. S.; Hayat, K.; He, J.; Hegazi, O. E.; Heidari, M.; Hezam, K.; Holla, R.; Holm, M.; Hopkins, H.; Hossain, M. M.; Hosseinzadeh, M.; Hostiuc, S.; Hussein, N. R.; Huy, L. D.; Ibáñez-Prada, E. D.; Ikiroma, A.; Ilic, I. M.; Islam, S. M. S.; Ismail, F.; Ismail, N. E.; Iwu, C. D.; Iwu-Jaja, C. J.; Jafarzadeh, A.; Jaiteh, F.; Jalilzadeh Yengejeh, R.; Jamora, R. D. G.; Javidnia, J.; Jawaid, T.; Jenney, A. W. J.; Jeon, H. J.; Jokar, M.; Jomehzadeh, N.; Joo, T.; Joseph, N.; Kamal, Z.; Kanmodi, K. K.; Kantar, R. S.; Kapisi, J. A.; Karaye, I. M.; Khader, Y. S.; Khajuria, H.; Khalid, N.; Khamesipour, F.; Khan, A.; Khan, M. J.; Khan, M. T.; Khanal, V.; Khidri, F. F.; Khubchandani, J.; Khusuwan, S.; Kim, M. S.; Kisa, A.; Korshunov, V. A.; Krapp, F.; Krumkamp, R.; Kuddus, M.; Kulimbet, M.; Kumar, D.; Kumaran, E. A. P.; Kuttikkattu, A.; Kyu, H. H.; Landires, I.; Lawal, B. K.; Le, T. T. T.; Lederer, I. M.; Lee, M.; Lee, S. W.; Lepape, A.; Lerango, T. L.; Ligade, V. S.; Lim, C.; Lim, S. S.; Limenh, L. W.; Liu, C.; Liu, X.; Liu, X.; Loftus, M. J.; M Amin, H. I.; Maass, K. L.; Maharaj, S. B.; Mahmoud, M. A.; Maikanti-Charalampous, P.; Makram, O. M.; Malhotra, K.; Malik, A. A.; Mandilara, G. D.; Marks, F.; Martinez-Guerra, B. A.; Martorell, M.; Masoumi-Asl, H.; Mathioudakis, A. G.; May, J.; McHugh, T. A.; Meiring, J.; Meles, H. N.; Melese, A.; Melese, E. B.; Minervini, G.; Mohamed, N. S.; Mohammed, S.; Mohan, S.; Mokdad, A. H.; Monasta, L.; Moodi Ghalibaf, A.; Moore, C. E.; Moradi, Y.; Mossialos, E.; Mougin, V.; Mukoro, G. D.; Mulita, F.; Muller-Pebody, B.; Murillo-Zamora, E.; Musa, S.; Musicha, P.; Musila, L. A.; Muthupandian, S.; Nagarajan, A. J.; Naghavi, P.; Nainu, F.; Nair, T. S.; Najmuldeen, H. H. R.; Natto, Z. S.; Nauman, J.; Nayak, B. P.; Nchanji, G. T.; Ndishimye, P.; Negoi, I.; Negoi, R. I.; Nejadghaderi, S. A.; Nguyen, Q. P.; Noman, E. A.; Nwakanma, D. C.; O'Brien, S.; Ochoa, T. J.; Odetokun, I. A.; Ogundijo, O. A.; Ojo-Akosile, T. R.; Okeke, S. R.; Okonji, O. C.; Olagunju, A. T.; Olivas-Martinez, A.; Olorukooba, A. A.; Olwoch, P.; Onyedibe, K. I.; Ortiz-Brizuela, E.; Osuolale, O.; Ounchanum, P.; Oyeyemi, O. T.; P A, M. P.; Paredes, J. L.; Parikh, R. R.; Patel, J.; Patil, S.; Pawar, S.; Peleg, A. Y.; Peprah, P.; Perdigão, J.; Perrone, C.; Petcu, I.-R.; Phommasone, K.; Piracha, Z. Z.; Poddighe, D.; Pollard, A. J.; Poluru, R.; Ponce-De-Leon, A.; Puvvula, J.; Qamar, F. N.; Qasim, N. H.; Rafai, C. D.; Raghav, P.; Rahbarnia, L.; Rahim, F.; Rahimi-Movaghar, V.; Rahman, M.; Rahman, M. A.; Ramadan, H.; Ramasamy, S. K.; Ramesh, P. S.; Ramteke, P. W.; Rana, R. K.; Rani, U.; Rashidi, M.-M.; Rathish, D.; Rattanavong, S.; Rawaf, S.; Redwan, E. M. M.; Reyes, L. F.; Roberts, T.; Robotham, J. V; Rosenthal, V. D.; Ross, A. G.; Roy, N.; Rudd, K. E.; Sabet, C. J.; Saddik, B. A.; Saeb, M. R.; Saeed, U.; Saeedi Moghaddam, S.; Saengchan, W.; Safaei, M.; Saghazadeh, A.; Saheb Sharif-Askari, N.; Sahebkar, A.; Sahoo, S. S.; Sahu, M.; Saki, M.; Salam, N.; Saleem, Z.; Saleh, M. A.; Samodra, Y. L.; Samy, A. M.; Saravanan, A.; Satpathy, M.; Schumacher, A. E.; Sedighi, M.;

Seekaew, S.; Shafie, M.; Shah, P. A.; Shahid, S.; Shahwan, M. J.; Shakoor, S.; Shalev, N.; Shamim, M. A.; Shamshirgaran, M. A.; Shamsi, A.; Sharifan, A.; Shastry, R. P.; Shetty, M.; Shittu, A.; Shrestha, S.; Siddig, E. E.; Sideroglou, T.; Sifuentes-Osornio, J.; Silva, L. M. L. R.; Simões, E. A. F.; Simpson, A. J. H.; Singh, A.; Singh, S.; Sinto, R.; Soliman, S. S. M.; Soraneh, S.; Stoesser, N.; Stoeva, T. Z.; Swain, C. K.; Szarpak, L.; T Y, S. S.; Tabatabai, S.; Tabche, C.; Taha, Z. M.-A.; Tan, K.-K.; Tasak, N.; Tat, N. Y.; Thaiprakong, A.; Thangaraju, P.; Tigoi, C. C.; Tiwari, K.; Tovani-Palone, M. R.; Tran, T. H.; Tumurkhuu, M.; Turner, P.; Udoakang, A. J.; Udoh, A.; Ullah, N.; Ullah, S.; Vaithinathan, A. G.; Valenti, M.; Vos, T.; Vu, H. T. L.; Waheed, Y.; Walker, A. S.; Walson, J. L.; Wangrangsimakul, T.; Weerakoon, K. G.; Wertheim, H. F. L.; Williams, P. C. M.; Wolde, A. A.; Wozniak, T. M.; Wu, F.; Wu, Z.; Yadav, M. K. K.; Yaghoubi, S.; Yahaya, Z. S.; Yarahmadi, A.; Yezli, S.; Yismaw, Y. E.; Yon, D. K.; Yuan, C.-W.; Yusuf, H.; Zakham, F.; Zamagni, G.; Zhang, H.; Zhang, Z.-J.; Zielińska, M.; Zumla, A.; Zyoud, S. H. H.; Zyoud, S. H.; Hay, S. I.; Stergachis, A.; Sartorius, B.; Cooper, B. S.; Dolecek, C.; Murray, C. J. L. Global Burden of Bacterial Antimicrobial Resistance 1990-2021: A Systematic Analysis with Forecasts to 2050. *Lancet* **2024**, *404* (10459), 1199–1226. https://doi.org/10.1016/S0140-6736(24)01867-1.

(3) Wang, G.; Li, X.; Wang, Z. APD3: The Antimicrobial Peptide Database as a Tool for Research and Education. *Nucleic Acids Res* **2016**, *44* (D1), D1087–D1093. https://doi.org/10.1093/nar/gkv1278.

(4) Magana, M.; Pushpanathan, M.; Santos, A. L.; Leanse, L.; Fernandez, M.; Ioannidis, A.; Giulianotti, M. A.; Apidianakis, Y.; Bradfute, S.; Ferguson, A. L.; Cherkasov, A.; Seleem, M. N.; Pinilla, C.; de la Fuente-Nunez, C.; Lazaridis, T.; Dai, T.; Houghten, R. A.; Hancock, R. E. W.; Tegos, G. P. The Value of Antimicrobial Peptides in the Age of Resistance. *Lancet Infect Dis* **2020**, *20* (9), e216–e230. https://doi.org/10.1016/S1473-3099(20)30327-3.

(5) Albin, J. S.; Lee, G. Y.; Johnson, C.; Vithanage, D. A.; Vuong, W.; Pentelute, B. L. Rapid Generation of Hypervariable Chemical Libraries. *Chem* **2025**, *0* (0), 102501. https://doi.org/10.1016/J.CHEMPR.2025.102501.

(6) Hancock, R. E. W.; Haney, E. F.; Gill, E. E. The Immunology of Host Defence Peptides: Beyond Antimicrobial Activity. *Nat Rev Immunol* **2016**, *16* (5), 321–334. https://doi.org/10.1038/nri.2016.29.

(7) Haney, E. F.; Straus, S. K.; Hancock, R. E. W. Reassessing the Host Defense Peptide Landscape. *Front Chem* **2019**, *7*, 43. https://doi.org/10.3389/fchem.2019.00043.

(8) Dürr, U. H. N.; Sudheendra, U. S.; Ramamoorthy, A. LL-37, the Only Human Member of the Cathelicidin Family of Antimicrobial Peptides. *Biochimica et Biophysica Acta (BBA) - Biomembranes* **2006**, *1758* (9), 1408–1425. https://doi.org/10.1016/J.BBAMEM.2006.03.030.

(9) Turner, J.; Cho, Y.; Dinh, N. N.; Waring, A. J.; Lehrer, R. I. Activities of LL-37, a Cathelin-Associated Antimicrobial Peptide of Human Neutrophils. *Antimicrob Agents Chemother* **1998**, *42* (9), 2206–2214.

(10) De Yang; Chen, Q.; Schmidt, A. P.; Anderson, G. M.; Wang, J. M.; Wooters, J.; Oppenheim, J. J.; Chertov, O. Ll-37, the Neutrophil Granule–And Epithelial Cell–Derived Cathelicidin, Utilizes Formyl Peptide Receptor–Like 1 (Fprl1) as a Receptor to Chemoattract Human Peripheral Blood

Neutrophils, Monocytes, and T Cells. *J Exp Med* **2000**, *192* (7), 1069–1074. https://doi.org/10.1084/jem.192.7.1069.

(11) Wan, M.; van der Does, A. M.; Tang, X.; Lindbom, L.; Agerberth, B.; Haeggström, J. Z. Antimicrobial Peptide LL-37 Promotes Bacterial Phagocytosis by Human Macrophages. *J Leukoc Biol* **2014**, *95* (6), 971–981. https://doi.org/10.1189/jlb.0513304.

(12) Mookherjee, N.; Lippert, D. N. D.; Hamill, P.; Falsafi, R.; Nijnik, A.; Kindrachuk, J.; Pistolic, J.; Gardy, J.; Miri, P.; Naseer, M.; Foster, L. J.; Hancock, R. E. W. Intracellular Receptor for Human Host Defense Peptide LL-37 in Monocytes. *The Journal of Immunology* **2009**, *183* (4), 2688–2696. https://doi.org/10.4049/jimmunol.0802586.

(13) De Yang, B.; Chen, Q.; Schmidt, A. P.; Anderson, G. M.; Wang, J. M.; Wooters, J.; Oppenheim, J. J.; Chertov, O. LL-37, the Neutrophil Granule- and Epithelial Cell-Derived Cathelicidin, Utilizes Formyl Peptide Receptor-like 1 (FPRL1) as a Receptor to Chemoattract Human Peripheral Blood Neutrophils, Monocytes, and T Cells. *Journal of Experimental Medicine* **2000**, *192* (7), 1069–1074. https://doi.org/10.1084/jem.192.7.1069.

(14) Cirioni, O.; Giacometti, A.; Ghiselli, R.; Bergnach, C.; Orlando, F.; Silvestri, C.; Mocchegiani, F.; Licci, A.; Skerlavaj, B.; Rocchi, M.; Saba, V.; Zanetti, M.; Scalise, G. LL-37 Protects Rats against Lethal Sepsis Caused by Gram-Negative Bacteria. *Antimicrob Agents Chemother* **2006**, *50* (5), 1672–1679. https://doi.org/10.1128/AAC.50.5.1672-1679.2006.

(15) Burton, M. F.; Steel, P. G. The Chemistry and Biology of LL-37. *Nat Prod Rep* **2009**, *26* (12), 1572–1584. https://doi.org/10.1039/B912533G.

(16) Spokoyny, A. M.; Zou, Y.; Ling, J. J.; Yu, H.; Lin, Y.-S.; Pentelute, B. L. A Perfluoroaryl-Cysteine S N Ar Chemistry Approach to Unprotected Peptide Stapling. **2013**. https://doi.org/10.1021/ja400119t.

(17) Mourtada, R.; Herce, H. D.; Yin, D. J.; Moroco, J. A.; Wales, T. E.; Engen, J. R.; Walensky, L. D. Design of Stapled Antimicrobial Peptides That Are Stable, Nontoxic and Kill Antibiotic-Resistant Bacteria in Mice. *Nat Biotechnol* **2019**, *37* (10), 1186–1197. https://doi.org/10.1038/s41587-019-0222-z.

(18) Schissel, C. K.; Farquhar, C. E.; Malmberg, A. B.; Loas, A.; Pentelute, B. L. Cell-Penetrating d -Peptides Retain Antisense Morpholino Oligomer Delivery Activity. *ACS Bio and Med Chem Au* **2022**, *2* (2), 150–160. https://doi.org/10.1021/ACSBIOMEDCHEMAU.1C00053/ASSET/IMAGES/MEDIUM/BG1C00053_M001.GIF.

(19) Srinivas, N.; Jetter, P.; Ueberbacher, B. J.; Werneburg, M.; Zerbe, K.; Steinmann, J.; Van der Meijden, B.; Bernardini, F.; Lederer, A.; Dias, R. L. A.; Misson, P. E.; Henze, H.; Zumbrunn, J.; Gombert, F. O.; Obrecht, D.; Hunziker, P.; Schauer, S.; Ziegler, U.; Käch, A.; Eberl, L.; Riedel, K.; DeMarco, S. J.; Robinson, J. A. Peptidomimetic Antibiotics Target Outer-Membrane Biogenesis in Pseudomonas Aeruginosa. *Science* **2010**, *327* (5968), 1010–1013. https://doi.org/10.1126/science.1182749.

(20) Martin-Loeches, I.; Dale, G. E.; Torres, A. Murepavadin: A New Antibiotic Class in the Pipeline. *Expert Rev Anti Infect Ther* **2018**, *16* (4), 259–268. https://doi.org/10.1080/14787210.2018.1441024.

(21) Wang, G. Structures of Human Host Defense Cathelicidin LL-37 and Its Smallest Antimicrobial Peptide KR-12 in Lipid Micelles. *Journal of Biological Chemistry* **2008**, *283* (47), 32637–32643. https://doi.org/10.1074/JBC.M805533200.

(22) Agerberth, B.; Gunne, H.; Odeberg, J.; Kogner, P.; Boman, H. G.; Gudmundsson, G. H. PR-39, a Proline-Rich Peptide Antibiotic from Pig, and FALL-39, a Tentative Human Counterpart. *Vet Immunol Immunopathol* **1996**, *54* (1–4), 127–131. https://doi.org/10.1016/S0165-2427(96)05676-0.

(23) Agerberth, B.; Gunne, H.; Odeberg, J.; Kogner, P.; Boman, H. G.; Gudmundsson, G. H. FALL-39, a Putative Human Peptide Antibiotic, Is Cysteine-Free and Expressed in Bone Marrow and Testis. *Proc Natl Acad Sci U S A* **1995**, *92* (1), 195–199. https://doi.org/10.1073/PNAS.92.1.195.

(24) Gudmundsson, G. H.; Magnusson, K. P.; Chowdhary, B. P.; Johansson, M.; Andersson, L.; Boman, H. G. Structure of the Gene for Porcine Peptide Antibiotic PR-39, a Cathelin Gene Family Member: Comparative Mapping of the Locus for the Human Peptide Antibiotic FALL-39. *Proceedings of the National Academy of Sciences* **1995**, *92* (15), 7085–7089. https://doi.org/10.1073/PNAS.92.15.7085.

(25) Gudmundsson, G. H.; Agerberth, B.; Odeberg, J.; Bergman, T.; Olsson, B.; Salcedo, R. The Human Gene FALL39 and Processing of the Cathelin Precursor to the Antibacterial Peptide LL-37 in Granulocytes. *Eur J Biochem* **1996**, *238* (2), 325–332. https://doi.org/10.1111/J.1432-1033.1996.0325Z.X.

(26) Wang, G.; Hanke, M. L.; Mishra, B.; Lushnikova, T.; Heim, C. E.; Thomas, V. C.; Bayles, K. W.; Kielian, T. Transformation of Human Cathelicidin LL-37 into Selective, Stable, and Potent Antimicrobial Compounds. *ACS Chem Biol* **2014**, *9* (9), 1997–2002. https://doi.org/10.1021/CB500475Y/SUPPL_FILE/CB500475Y_SI_001.PDF.

(27) Li, X.; Li, Y.; Han, H.; Miller, D. W.; Wang, G. Solution Structures of Human Ll-37 Fragments and NMR-Based Identification of a Minimal Membrane-Targeting Antimicrobial and Anticancer Region. *J Am Chem Soc* **2006**, *128* (17), 5776–5785. https://doi.org/10.1021/JA0584875/SUPPL_FILE/JA0584875SI20051222_013003.PDF.

(28) *CLSI eClipse Ultimate Access - Powered by Edaptive Technologies*. https://em100.edaptivedocs.net/Login.aspx?ru=1&emsg=275 (accessed 2025-05-07).

(29) Tai, K. P.; Le, V. V.; Selsted, M. E.; Ouellette, A. J. Hydrophobic Determinants of α-Defensin Bactericidal Activity. *Infect Immun* **2014**, *82* (6), 2195–2202. https://doi.org/10.1128/IAI.01414-13.

(30) Dean, S. N.; Bishop, B. M.; Van Hoek, M. L. Susceptibility of Pseudomonas Aeruginosa Biofilm to Alpha-Helical Peptides: D-Enantiomer of LL-37. *Front Microbiol* **2011**, *2* (JULY), 10301. https://doi.org/10.3389/FMICB.2011.00128/BIBTEX.

(31) Kim, E. Y.; Rajasekaran, G.; Shin, S. Y. LL-37-Derived Short Antimicrobial Peptide KR-12-A5 and Its D-Amino Acid Substituted Analogs with Cell Selectivity, Anti-Biofilm Activity, Synergistic Effect with Conventional Antibiotics, and Anti-Inflammatory Activity. *Eur J Med Chem* **2017**, *136*, 428–441. https://doi.org/10.1016/j.ejmech.2017.05.028.

(32) Kamysz, E.; Sikorska, E.; Jaśkiewicz, M.; Bauer, M.; Neubauer, D.; Bartoszewska, S.; Barańska-Rybak, W.; Kamysz, W. Lipidated Analogs of the Ll-37-Derived Peptide Fragment KR12—Structural Analysis, Surface-Active Properties and Antimicrobial Activity. *Int J Mol Sci* **2020**, *21* (3). https://doi.org/10.3390/ijms21030887.

(33) Kamysz, E.; Sikorska, E.; Bauer, M.; Sikora, K.; Neubauer, D. Influence of Lipidation Pattern of the KR12 Fragment of Peptide LL-37 on Its Antibacterial and Hemolytic Activities. *Int J Mol Sci* **2023**, *24* (6), 5505. https://doi.org/10.3390/IJMS24065505/S1.

(34) Wang, Z.; Koirala, B.; Hernandez, Y.; Zimmerman, M.; Park, S.; Perlin, D. S.; Brady, S. F. A Naturally Inspired Antibiotic to Target Multidrug-Resistant Pathogens. *Nature 2022 601:7894* **2022**, *601* (7894), 606–611. https://doi.org/10.1038/s41586-021-04264-x.

(35) Quartararo, A. J.; Gates, Z. P.; Somsen, B. A.; Hartrampf, N.; Ye, X.; Shimada, A.; Kajihara, Y.; Ottmann, C.; Pentelute, B. L. Ultra-Large Chemical Libraries for the Discovery of High-Affinity Peptide Binders. *Nat Commun* **2020**, *11* (1), 1–11. https://doi.org/10.1038/s41467-020-16920-3.

(36) Wiegand, I.; Hilpert, K.; Hancock, R. E. W. Agar and Broth Dilution Methods to Determine the Minimal Inhibitory Concentration (MIC) of Antimicrobial Substances. *Nat Protoc* **2008**, *3* (2), 163–175. https://doi.org/10.1038/nprot.2007.521.

(37) Albin, J. S.; Pentelute, B. L. Efficient Flow Synthesis of Human Antimicrobial Peptides. *Aust J Chem* **2020**, *73* (4), 380–388. https://doi.org/10.1071/CH20043.

(38) Hartrampf, N.; Saebi, A.; Poskus, M.; Gates, Z. P.; Callahan, A. J.; Cowfer, A. E.; Hanna, S.; Antilla, S.; Schissel, C. K.; Quartararo, A. J.; Ye, X.; Mijalis, A. J.; Simon, M. D.; Loas, A.; Liu, S.; Jessen, C.; Nielsen, T. E.; Pentelute, B. L. Synthesis of Proteins by Automated Flow Chemistry. *Science (1979)* **2020**, *368* (6494), 980–987. https://doi.org/10.1126/science.abb2491.

(39) Mijalis, A. J.; Thomas, D. A.; Simon, M. D.; Adamo, A.; Beaumont, R.; Jensen, K. F.; Pentelute, B. L. A Fully Automated Flow-Based Approach for Accelerated Peptide Synthesis. *Nat Chem Biol* **2017**, *13* (5), 464–466. https://doi.org/10.1038/nchembio.2318.

(40) Simon, M. D.; Heider, P. L.; Adamo, A.; Vinogradov, A. A.; Mong, S. K.; Li, X.; Berger, T.; Policarpo, R. L.; Zhang, C.; Zou, Y.; Liao, X.; Spokoyny, A. M.; Jensen, K. F.; Pentelute, B. L. Rapid Flow-Based Peptide Synthesis. *ChemBioChem* **2014**, *15* (5), 713–720. https://doi.org/10.1002/cbic.201300796.

A.

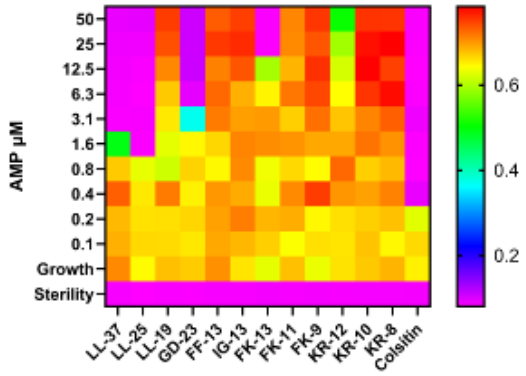

B.

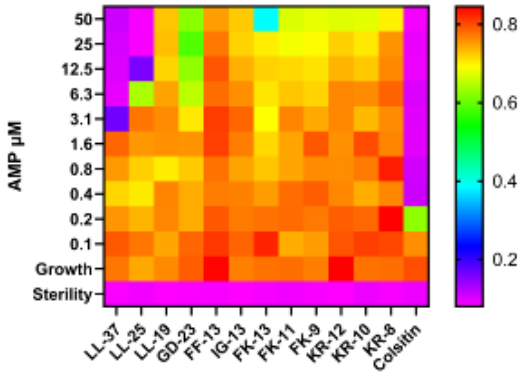

C.

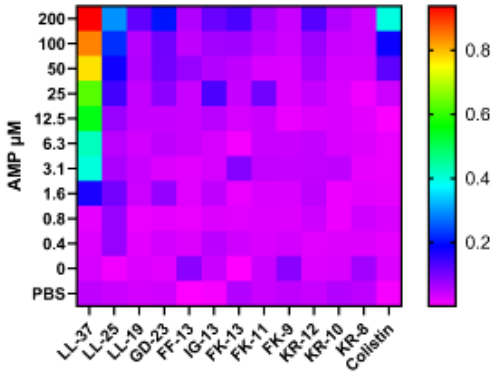

D.

```
LL-37     LLGDFFRKSKEKIGKEFKRIVQRIKDFLRNLVPRTES   37
LL-25     LLGDFFRKSKEKIGKEFKRIVQRIK------------   25
LL-19     LLGDFFRKSKEKIGKEFKR-------------------   19
GD-23     --GDFFRKSKEKIGKEFKRIVQRIK------------   23
FF-13     ----FFRKSKEKIGKEF---------------------   13
IG-13     ------------IGKEFKRIVQRIK------------   13
FK-13     -----------------FKRIVQRIKDFLR--------   13
FK-11     -----------------FKRIVQRIKDF----------   11
FK-9      -----------------FKRIVQRIK------------   9
KR-12     ------------------KRIVQRIKDFLR--------   12
KR-10     ------------------KRIVQRIKDF----------   10
KR-8      ------------------KRIVQRIK------------   8
```

Figure 1 – Limited activity of shorter derivatives of LL-37. A. Antimicrobial susceptibility testing showing the activity of each derivative as well as a colistin control for reference against *E. coli* (ATCC 25922). In the heatmap plate depiction, cooler colors indicate low or absent bacterial growth as detected by the OD600 measured at 18 hours of incubation at 37 °C. **B.** As in **A.**, but with *Pseudomonas aeruginosa* (ATCC 27853). **C.** Hemolysis assays in which defibrinated sheep blood in PBS was incubated with the indicated peptide for 18 hours at 37 °C with subsequent quantification of hemoglobin released into the supernatant at 414 nm. Cool colors indicate little or no release of hemoglobin, where all levels are scaled to 100% hemolysis freeze-thaw controls. Levels throughout are the mean of three independent experiments. **D.** Alignment showing the sequence of LL-37 in comparison with shorter derivatives tested in initial studies, which have been described previously.

A.

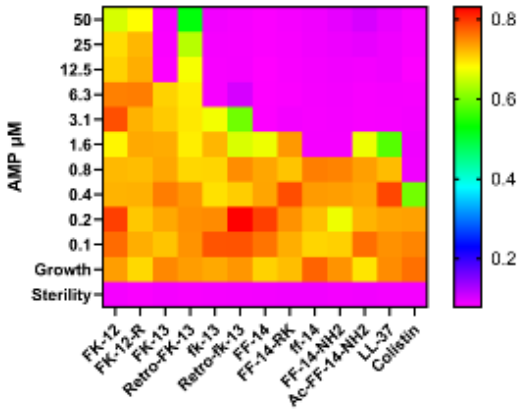

B.

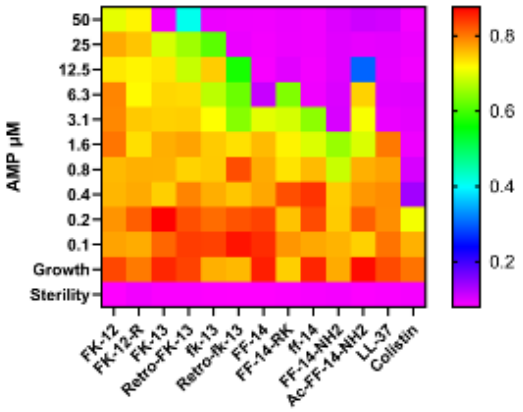

C.

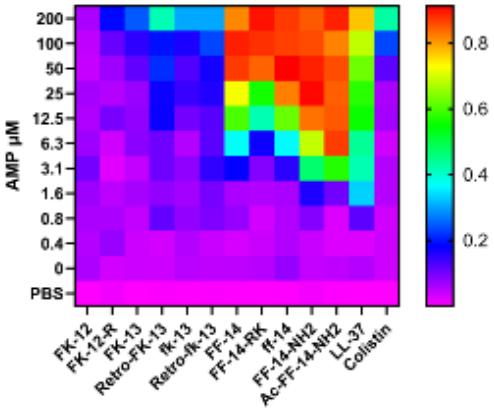

D.

FK-12	-FKRIVQRIKDFL
FK-12-R	-FKRIVQRIKDF-R
FK-13	-FKRIVQRIKDFLR
Retro-FK-13	-RLFDKIRQVIRKF
fk-13	-fkrivqrikdflr
Retro fk-13	-rlfdkirqvirkf
FF-14	FFKRIVQRIKDFLR
FF-14-RK	FFRKIVQRIKDFLR
ff-14	ffkrivqrikdflr
FF-14-NH_2	FFKRIVQRIKDFLR-NH_2
Ac-FF-14-NH_2	Ac-FFKRIVQRIKDFLR-NH_2
LL-37	LLGD**FFRK**SKEKIGK**EFKR**IVQRIKDFLRNLVPRTES

Figure 2 – Mimicry of the LL-37 N-terminus yields a 14-mer with activity comparable to full-length LL-37. A. Antimicrobial susceptibility testing showing the activity of each derivative as well as a colistin control against *E. coli* (ATCC 25922). In the heatmap plate depiction, cooler colors indicate low or absent bacterial growth as detected by the OD600 measure at 18 hours of incubation at 37 °C. **B.** As in **A.**, but with *Pseudomonas aeruginosa* (ATCC 27853). **C.** Endpoint hemolysis assays with defibrinated sheep blood following incubation with the indicated peptide for 18 hours at 37 °C with subsequent quantification of supernatant free hemoglobin at 414 nm. Cool colors indicate little or no release of hemoglobin. Levels throughout are the mean of three independent experiments. **D.** Alignment showing the sequence of LL-37 in comparison with shorter derivatives tested in these studies. The FF[RK] region transposed to the central activity region on which KR-12 and FK-13 are built is shown in bold with highlighting.

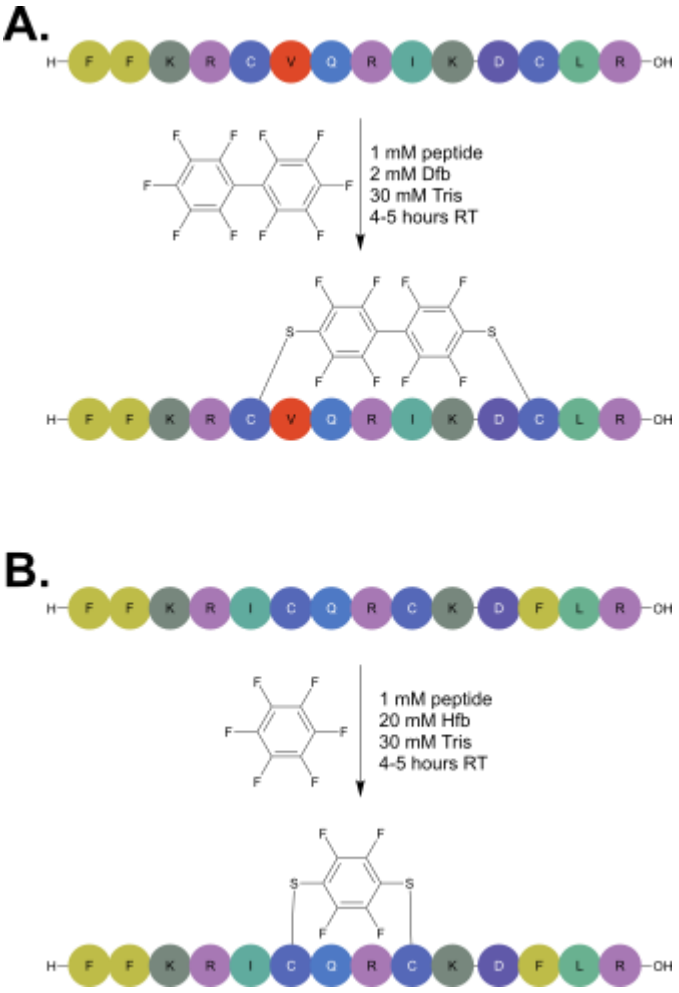
A.
H F F K R C V Q R I K D C L R OH
1 mM peptide
2 mM Dfb
30 mM Tris
4-5 hours RT
B.
H F F K R I C Q R C K D F L R OH
1 mM peptide
20 mM Hfb
30 mM Tris
4-5 hours RT

Figure 3 – General scheme for cysteine perfluoroarylation. A. Schematic showing conditions for stapling of *i,i+7* positions with decafluorobiphenyl. **B.** Schematic showing conditions for stapling of *i,i+3* or *i,i+4* positions with hexafluorobenzene.

A.

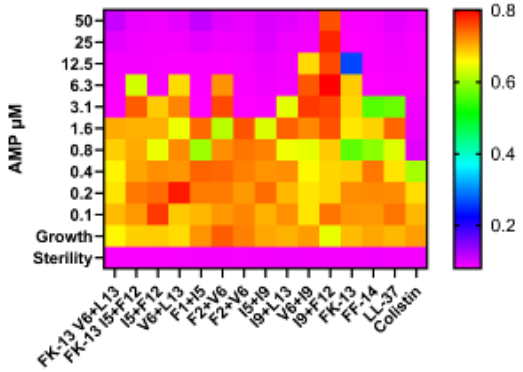

B.

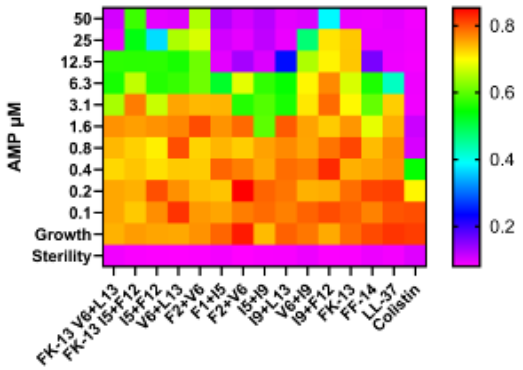

C.

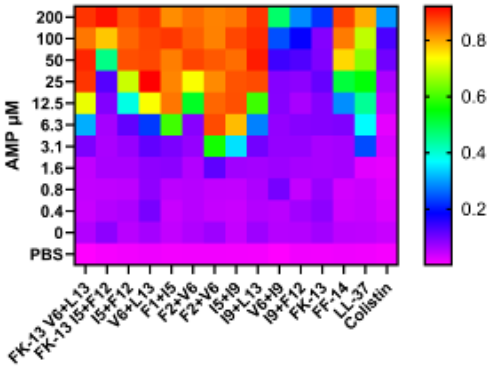

D.

FK-13 6+13	-FKRI**C**QRIKDF**C**R
FK-13 5+12	-FKR**C**VQRIKD**C**LR
I5+F12	FFKR**C**VQRIKD**C**LR
V6+L13	FFKRI**C**QRIKDF**C**R
F1+I5	**C**FKR**C**VQRIKDFLR
F2+V6	F**C**KRI**C**QRIKDFLR
F2+V6	F**C**KRI**C**QRIKDFLR
I5+I9	FFKR**C**VQR**C**KDFLR
I9+L13	FFKRIVQR**C**KDF**C**R
V6+I9	FFKRI**C**QR**C**KDFLR
I9+F12	FFKRIVQR**C**KD**C**LR
FK-13	-FKRIVQRIKDFLR
FF-14	FFKRIVQRIKDFLR

Figure 4 – Perfluoroaryl stapling yields antimicrobial activity changes that track with hemolytic activity. A. Antimicrobial susceptibility testing showing the activity of each derivative against *E. coli* (ATCC 25922). In the heatmap plate depiction, cooler colors indicate low or absent bacterial growth as detected by the OD600 measure at 18 hours of incubation at 37 °C. **B.** As in **A.**, but with *Pseudomonas aeruginosa* (ATCC 27853). **C.** Endpoint hemolysis assays in which sheep RBCs in PBS were incubated with the indicated peptide for 18 hours at 37 °C. Cool colors indicate little or no release of hemoglobin as measured at 414 nm, where all levels are scaled to 100% hemolysis freeze-thaw controls. Levels throughout are the mean of three independent experiments. **D.** Alignment showing the stapled Cys residues used in each derivative.

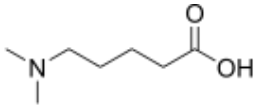

5-Dimethylamino-pentanoic Acid

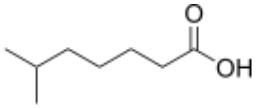

6-methyl-heptanoic acid

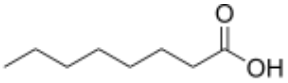

Octanoic Acid

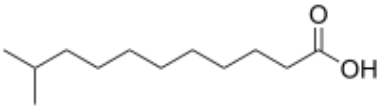

10-Methylundecanoic acid

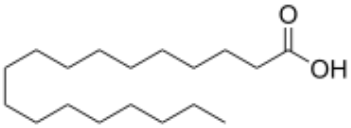

Stearic Acid

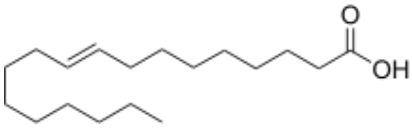

Elaidic Acid

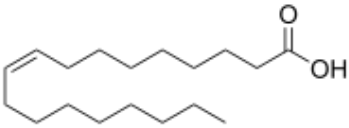

Oleic Acid

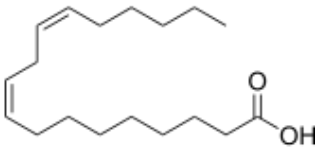

Linoleic Acid

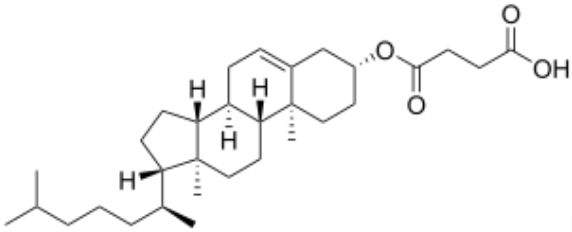

Cholesteryl Hemisuccinate

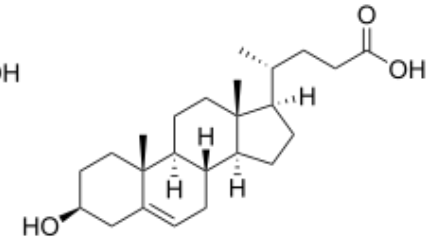

Cholenic Acid

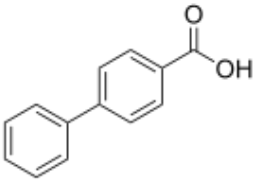

Biphenyl-4-carboxylic Acid

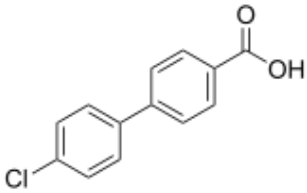

4-Chloro-biphenyl-4-carboxylic Acid

Figure 5 – N-terminal lipidation moieties used in this study. Structures of the lipid tails appended to the N-terminus of FF-14 are shown.

A.

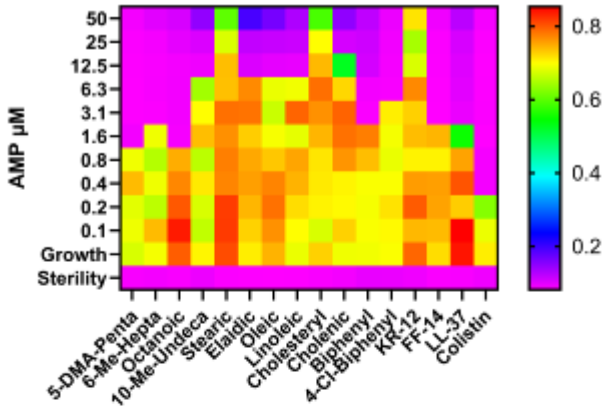
AMP µM
50
25
12.5
6.3
3.1
1.6
0.8
0.4
0.2
0.1
Growth
Sterility
5-DMA-Penta
6-Me-Hepta
Octanoic
10-Me-Undeca
Stearic
Elaidic
Oleic
Linoleic
Cholesteryl
Cholenic
Biphenyl
4-Cl-Biphenyl
KR-12
FF-14
LL-37
Colistin
0.8
0.6
0.4
0.2

B.

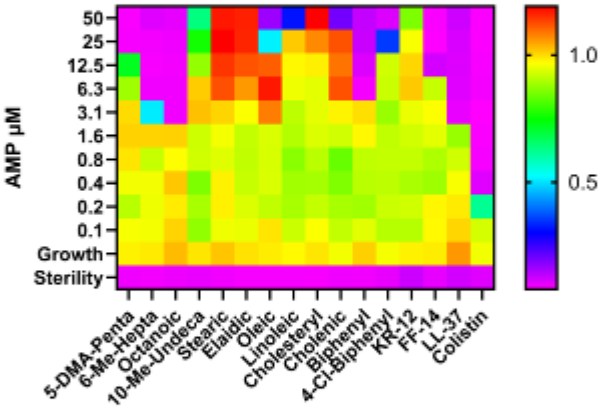
AMP µM
50
25
12.5
6.3
3.1
1.6
0.8
0.4
0.2
0.1
Growth
Sterility
5-DMA-Penta
6-Me-Hepta
Octanoic
10-Me-Undeca
Stearic
Elaidic
Oleic
Linoleic
Cholesteryl
Cholenic
Biphenyl
4-Cl-Biphenyl
KR-12
FF-14
LL-37
Colistin
1.0
0.5

C.

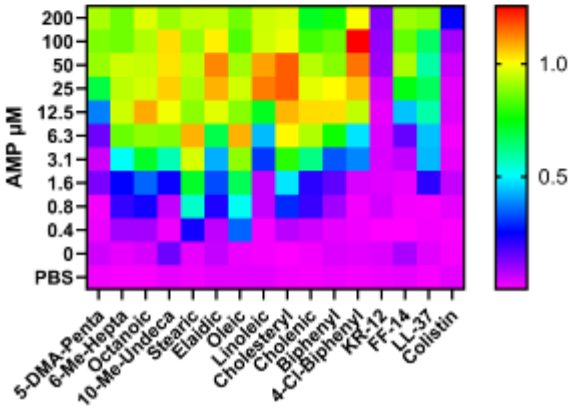
AMP µM
200
100
50
25
12.5
6.3
3.1
1.6
0.8
0.4
0
PBS
5-DMA-Penta
6-Me-Hepta
Octanoic
10-Me-Undeca
Stearic
Elaidic
Oleic
Linoleic
Cholesteryl
Cholenic
Biphenyl
4-Cl-Biphenyl
KR-12
FF-14
LL-37
Colistin
1.0
0.5

Figure 6 – Variable effects of N-terminal lipidation moieties on FF-14 activity. B. Antimicrobial susceptibility testing showing the activity of each derivative as well as a colistin control against *E. coli* (ATCC 25922). In the heatmap plate depiction, cooler colors indicate low or absent bacterial growth as detected by the OD600 measure at 18 hours of incubation at 37 °C. **B.** As in **A.**, but with *Pseudomonas aeruginosa* (ATCC 27853). **C.** Endpoint hemolysis assay following 18 hours of incubation with the indicated derivative at 37 °C. Cool colors indicate little or no release of hemoglobin. Levels throughout are the mean of three independent experiments.